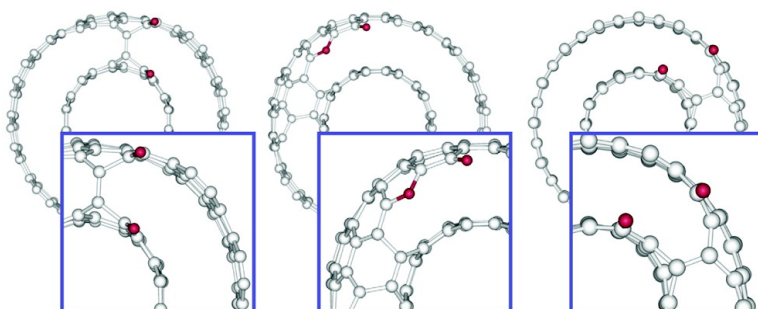


Oxygen Gas-Induced Lip–Lip Interactions on a Double-Walled Carbon Nanotube Edge

Yong Soo Choi, Kyung Ah Park, Changwook Kim, and Young Hee Lee

J. Am. Chem. Soc., **2004**, 126 (30), 9433-9438 • DOI: 10.1021/ja039917z • Publication Date (Web): 09 July 2004

Downloaded from <http://pubs.acs.org> on April 1, 2009



More About This Article

Additional resources and features associated with this article are available within the HTML version:

- Supporting Information
- Access to high resolution figures
- Links to articles and content related to this article
- Copyright permission to reproduce figures and/or text from this article

[View the Full Text HTML](#)

Oxygen Gas-Induced Lip–Lip Interactions on a Double-Walled Carbon Nanotube Edge

Yong Soo Choi,[†] Kyung Ah Park,[†] Changwook Kim,[‡] and Young Hee Lee^{*†}

Contribution from the Department of Physics, Institute of Basic Science, Center for Nanotubes and Nanostructured Composites, Sungkyunkwan University, Suwon 440-746, Korea, and CAE Team, Corporate R&D Center, Samsung SDI Co., LTD, Yongin, 449-577, Korea

Received December 3, 2003; E-mail: leeyoung@skku.edu

Abstract: We have investigated adsorption of an O₂ molecule on a double-walled carbon nanotube (DWCNT) edge using density functional theory calculations. An O₂ molecule adsorbs exothermally without an adsorption barrier at open nanotube edges that are energetically favorable with a large adsorption energy of about −9 eV in most cases. Dissociative adsorption of an O₂ molecule induces various spontaneous lip–lip interactions via the bridged carbon atoms, generating the closed tube ends. This explains why the DWCNTs are chemically more stable than the single-walled nanotubes during observed field emission experiments. The field emission takes place via the localized states of the bridged carbon atoms, not via those of the adsorbed oxygen atoms particularly in the armchair nanotubes. We also find that some O₂ precursor states exist as a bridge between tube edges.

Introduction

Oxygen molecule is one of the important ambient gases that play an essential role in many aspects of carbon nanotubes (CNTs). The presence of oxygen gases on the nanotube wall induces a charge transfer from nanotube to adsorbate, creating a hole-type charge carrier in the nanotube.^{1,2} They also modify the work function of the metal-nanotube contact which governs the transport properties of the nanotube transistors.³ Oxygen gases have been also used for purification of carbon nanotubes, where the carbonaceous particles were selectively removed by an oxidative etching.^{4–6} The presence of oxygen gases on the tube edge not only reduces the field emission currents but also induces severe tip degradation.^{7–9} Recently the double-walled carbon nanotube (DWCNT) has been suggested for an ultimate CNT tip due to their small diameter (larger field enhancement factor similar to those of single-walled nanotubes (SWCNTs)) and the high tip stability comparable to the multiwalled nanotubes (MWCNT).¹⁰

Despite such demands of intensive researches for oxygen adsorbates on SWCNTs and DWCNTs from experiment, theoretical models are rare. A selective etching of amorphous carbons from SWCNTs by oxygen gases has been successfully described.⁶ Unlike strong chemisorption of oxygen molecules on CNT edges, physisorption of O₂ molecule on the tube wall depends strongly on the spin states.¹¹ Yet, no theoretical model for O₂ adsorption on the DWCNT edges has been reported. Moreover, the advantage of this model for DWCNTs can be further extended to explain the physical and chemical properties of MWCNTs.

The issue in this report is to build a theoretical model for gas adsorption, particularly oxygen molecules on the open DWCNT edge and possibly to see its field emission characteristics, which might be different from those of the SWCNT edge. We find that an oxygen molecule adsorbs at the edge of an inner or outer wall exothermally with a large adsorption energy and, more importantly, induces a cap closure of the edge atoms, leading to spontaneous lip–lip interactions via the bridged carbon atoms. We also find some bridged O₂ precursor states between two edges. The Fermi level is shifted down toward the valence band, but its shift is much less than that of the SWCNT, giving rise to less severe degradation in the emission currents. The localized energy levels of the adsorbed oxygen atoms are far below the Fermi level and do not contribute to the field emission currents.

Result and Discussion

Theoretical Approaches. For our calculations we use a self-consistent charge-density-functional-based tight-binding (SCC-

[†] Sungkyunkwan University.

[‡] Samsung SDI, Suwon, Korea.

- (1) Collins, P. G.; Bradley, K.; Ishigami, M.; Zettl, A. *Science* **2000**, *287*, 1801–1804.
- (2) Kong, J.; Franklin, N. R.; Zhou, C.; Chapline, M. G.; Peng, S.; Cho, K.; Dai, H. *Science* **2000**, *287*, 622–625.
- (3) Heinze, S.; Tersoff, J.; Martel, R.; Derycke, V.; Appenzeller, J.; Avouris, P. *Phys. Rev. Lett.* **2002**, *89*, 106801.
- (4) Moon, J. M.; Park, Y. S.; An, K. H.; Park, G. S.; Lee, Y. H. *J. Phys. Chem. B* **2001**, *105*, 5677.
- (5) Chiang, I. W.; Brinson, B. E.; Smalley, R. E.; Margrave, J. L.; Hauge, R. H. *J. Phys. Chem. B* **2001**, *105*, 1157.
- (6) Zhu, X. Y.; Lee, S. M.; Lee, Y. H.; Frauenheim, T. *Phys. Rev. Lett.* **2000**, *85*, 2757–2760.
- (7) Dean, K. A.; Chalamala, B. R. *Appl. Phys. Lett.* **1999**, *75*, 3017.
- (8) Lim, S. C.; Choi, Y. C.; Jeong, H. J.; Shin, Y. M.; Bae, D. J.; Lee, Y. H.; Lee, N. S.; Kim, J. M. *Adv. Mater.* **2001**, *13*, 1563.
- (9) Kim, C. W.; Choi, Y. S.; Lee, S. M.; Park, J. T.; Kim, B. S.; Lee, Y. H. *J. Am. Chem. Soc.* **2002**, *124*, 9906.
- (10) Uemura, S.; Yotani, J.; Nagasako, T.; Kurachi, H.; Yamada, H.; Ezaki, T.; Maesoba, T.; Nakao, T.; Saito, Y.; Yumura, M. *SID'02 Digest* **2002**, 1132.

- (11) Chan, S. P.; Chen, G.; Gong, X. G.; Liu, Z.-F. *Phys. Rev. Lett.* **2003**, *90*, 86403.

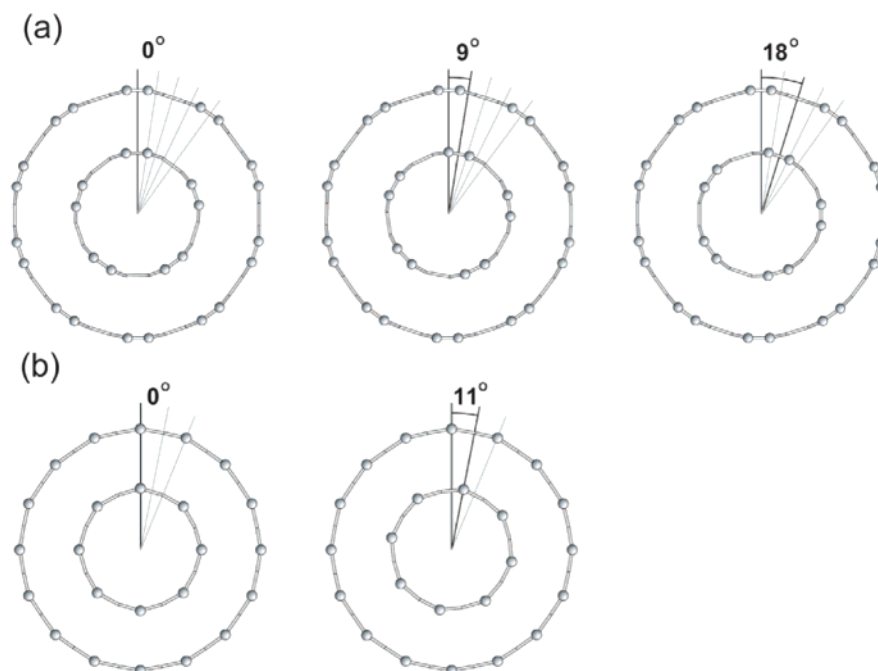


Figure 1. Top view in ball-and-stick model for the definition of relative orientations between inner and outer tubes for (a) (5,5)@(10,10) armchair and (b) (8,0)@(16,0) zigzag DWCNTs. The repetition angle is 36° in an armchair tube, which gives three different angles of 0° , 9° , and 18° , whereas, in zigzag tubes, the repetition angle is 22° , which gives two different angles of 0° and 11° .

DFTB) method¹² and linear combination of atomic orbitals (LCAO) basis set DF calculations within local-density approximation (LDA).¹³ The SCC-DFTB method uses a basis of numerically described s and p atomic orbitals for a carbon atom and s orbital for a hydrogen atom. Charge transfer is taken into account through an incorporation of a self-consistency scheme for Mulliken charges based on the second-order expansion of the Kohn–Sham energy in terms of charge density fluctuations. The diagonal elements of the Hamiltonian matrix employed are then modified by the charge-dependent contributions in order to describe the change in the atomic potentials due to the charge transfer. The off-diagonal elements have additional charge-dependent terms due to the Coulomb potential of ions. They decay as $1/r$ and thus account for the Madelung energy of the system. This procedure optimizes not only the total energy but also an excess charge transfer that is usually overestimated in a conventional tight-binding approach. Further detail of the SCC-DFTB method has been published elsewhere.¹² The exchange-correlation energy in LDA is parametrized by the Perdew and Wang’s scheme.¹⁴ All-electron Kohn–Sham wave functions are expanded in an LCAO basis set with each basis function that is defined numerically on an atomic-centered spherical-polar mesh. We use a double numeric polarized basis set, where the 2s and 2p carbon orbitals are represented by two wave functions each, and a 3d type wave function on each carbon atom is used to describe the polarization. No frozen core approximation is used throughout the calculations. Both calculations are done using an appropriately chosen cluster without a periodic boundary condition.

For our calculations, we choose the double-walled (5,5)@(10,10) and (8,0)@(16,0) nanotubes with respective inner diameters of 7.1 and 6.5 Å and an average bond length of 1.42

Å between the adjacent carbon atoms. The tube–tube distances are 3.4 and 3.2 Å, respectively, which are in the range of typical van der Waals interactions. We use eight carbon layers along the tube axis (z-axis) for armchair and zigzag tubes. The bottom dangling bonds are saturated by hydrogen atoms to minimize the edge effect. Open-ended tips are chosen in our calculations to see an adsorption effect. We define an adsorption energy of an O₂ molecule as $E_{\text{ad}}(\text{O}_2) = E_{\text{tot}}(\text{O}_2 + \text{CNT}) - E_{\text{tot}}(\text{O}_2) - E_{\text{tot}}(\text{CNT})$, where E_{tot} is the total energy of a given system. We choose an O₂ molecular state as a reference, similar to the previous reports.^{15,16} The forces on each atom to be converged during each relaxation are less than 10^{-3} au. Atoms are fully relaxed by a conjugate gradient method in the SCC-DFTB calculations except the bottom two carbon layers and hydrogen layer. More accurate calculations are done with the LDA approach whenever necessary.

Theoretical Model. We first define the relative orientation of two tube walls, as shown in Figure 1. The repetition units are 36° and 22° in armchair and zigzag tubes, respectively. We consider five different orientations in our calculations: 0° , 9° , and 18° in the armchair tube and 0° and 11° in the zigzag tube. Although there can be more detailed orientations, we believe that the current choices of orientations are the most representative to extract information for adsorption behavior on these tube edges. An oxygen molecule can be adsorbed on these edges with two different orientations: the molecular axis parallel and perpendicular to the radial direction. For a chosen orientation of tubes and oxygen molecule, we consider several different positions of oxygen adsorption.

Adsorption of O₂ Molecule. An oxygen molecule is initially placed between two tubes with a least separation distance of about 2 Å above from the closest carbon atom at the edge in

(12) Elstner, M.; Shuhai, S.; Seifert, G. *Phys. Rev. B* **1998**, *58*, 7260.

(13) DMol3 is a registered software product of Molecular Simulations Inc.

(14) Perdew, J. P.; Wang, Y. *Phys. Rev. B* **1992**, *45*, 13244.

(15) Maiti, A.; Andzelm, J.; Tanpipat, N.; van Allmen, P. *Phys. Rev. Lett.* **2001**, *87*, 15502.

(16) Park, N.; Han, S.; Ihm, J. *Phys. Rev. B* **2001**, *64*, 125401.

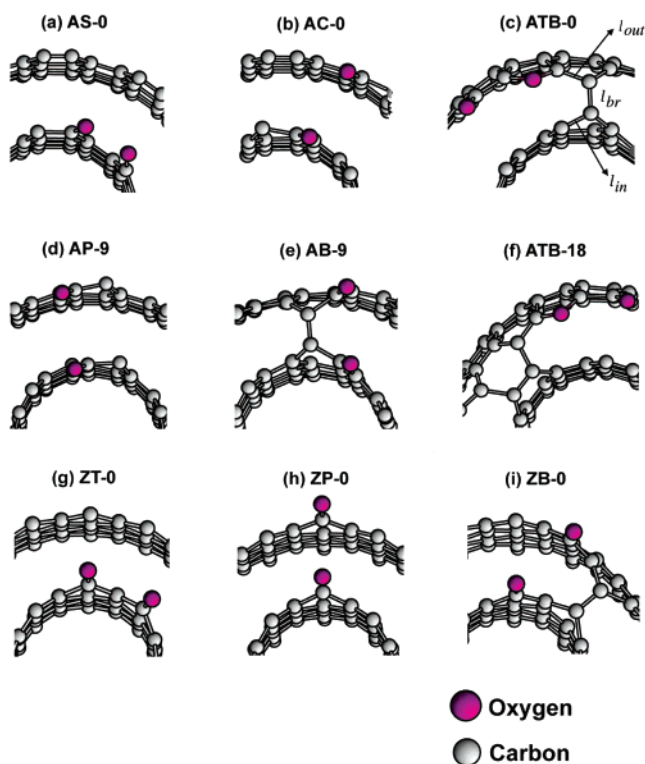


Figure 2. Bird's eye view of adsorption geometries of an O₂ molecule on (5,5)@(10,10) armchair DWCNT edges at (a) the "seat" site at the same tube edge, (b) "crossed" sites at different tube edges, (c) the "top-bridge" site across the tube edges, (d) "parallel" sites on both tube edges, (e) the "bridge" site at 9°, and (f) the "top-bridge" site at 18°. Adsorption geometries of an O₂ molecule on (8,0)@(16,0) zigzag DWCNT edges at (g) two "top" sites at the same tube edge, (h) "parallel" sites at different tube edges, and (i) the "bridge" site across tube edges.

various orientations, as described in the following. All atoms are fully relaxed except the bottom three layers. Figure 2 illustrates the typical stable adsorption geometries of an oxygen molecule among all geometries we tried. Figure 2a is a reference geometry, where an O₂ molecule is adsorbed exothermically on the seat site at the inner armchair tube with an adsorption energy of -5.33 eV, similar to the previous calculations.⁶ Adsorption at the outer wall gives a similar adsorption energy. When an oxygen molecule is placed between two tube edges with its axis of about 45° rotated from the radial direction, it dissociates exothermically into two oxygen atoms and forms strong bonds at the crossed inner and outer top sites, as shown in Figure 2b. The adsorption is slightly enhanced compared to Figure 2a due to the reduction of O–O repulsive force, resulting in larger Mulliken charge transfer, as listed in Table 1.

An interesting adsorption geometry is obtained when an O₂ molecule was adsorbed at one pentagon site and one top site via several intermediate states at the outer nanotube as described previously in Figure 2c.⁶ Formation of a pentagon at the carbon edge of SWCNT bends the tube edge inward in general, leading to a cap formation.^{17,18} Similarly, adsorption of an oxygen atom at the pentagon site of DWCNT bends the tube edge inward. This leads to spontaneous lip–lip interactions between two adjacent carbon atoms at the inner and outer top sites to form a bridge. The edge is stabilized by removing two dangling bonds at the top sites and instead forming a strong double bond (l_{br})

Table 1. Various Optimized Parameters from the SCC-DFTB Calculations^a

type	E_{ad} (eV)	l_{br} (Å)	l_{CO} (Å)	l_{in}, l_{out} (Å)	δC (e)
AS-0	-5.33		1.22		-0.27
AC-0	-5.44		1.22		-0.33
ATB-0	-9.20 (-10.83)	1.42	1.23 ^(T)	1.44, 1.47	-0.38 ^(T)
AP-9	-5.45		1.22		-0.34
AB-9	-9.05 (-10.58)	1.37	1.20	1.55, 1.52	-0.34
ATB-18	-10.88 (-11.60)	1.49	1.23 ^(T)	1.51, 1.42	-0.36 ^(T)
ZT-0	-8.32		1.20		-0.33
ZP-0	-8.74		1.20		-0.32
ZB-0	-9.91 (-11.32)	1.39	1.21	1.52, 1.47	-0.35

^a E_{ad} is an adsorption energy defined in the text. The values in the parentheses are from LDA calculations. The respective l_{br} and l_{CO} are the bond lengths between bridged carbon atoms and between carbon and oxygen atom. l_{in} and l_{out} are bond lengths between the carbon atom in the wall and the bridged carbon atoms at the inner and outer walls, respectively. "T" in the parentheses stands for the top site. δC (e) is the amount of excess charges at oxygen atom in electron units

in the bridge with a bond length of 1.42 Å, as indicated in Figure 2c. Formation of lip–lip interactions via the bridged atoms still retains hexagons in the two tube walls, minimizing the bond angle distortion energy. The bond lengths (l_{in} and l_{out}) between the bridged carbon atom and the carbon atoms in the tube wall are 1.54 and 1.52 Å, extended to a single bond. The energy gain is very significant with an adsorption energy of -9.2 eV compared to the AS-0 and AC-0 models. In case of 9° orientation, we also find geometries similar to those of zero angle orientation. Figure 2d shows a relaxed geometry when O₂ molecule was placed above the edge of the same top sites with the molecular axis parallel to the radial direction. No lip–lip interaction is induced in this case. The situation is different when one oxygen atom in O₂ molecule was placed in the middle of the top dimer at the inner wall and another oxygen atom at the top site of the outer wall with the molecular axis to be parallel to the radial direction (Figure 2e). Figure 3a shows energetics of the concerted adsorption pathways. These pathways are different from the dynamical pathways at finite temperature but provide an intuitive picture for energetics. The oxygen atom near the outer wall pulls up one of the top dimer carbon atoms and moves to the next top sites of the inner wall, as shown in step (ii). This process severely distorts another carbon atom in the same dimer of the outer wall, making them close to each other. The energy gain is still large with about -4 eV due to strong bonds between carbon and oxygen atoms. This induces the lip–lip interactions via the bridged carbon atoms, as shown in step (iii) in Figure 3a. One interesting point to note is that the O–O bond is dissociated completely once the C–C bond is bridged between two walls.

The energy gain is -9.05 eV, very large due to a complete hexagonal carbon network near the bridged carbon dimers, as shown in Figure 2e. The local geometries and adsorption energy are very similar to those in Figure 2c. In addition to these geometries, we obtain several stable geometries at 9°, which are similar to those obtained at zero orientation angle. We find another stable geometry (ATB-18) at 18° orientation, as shown in Figure 2f, when one of the oxygen atoms was placed at the pentagon site and another at the top site, similar to Figure 2c. In this case, however, the proximate dimers at the inner and outer walls induce the bridged hexagon formation. The energetics of this process is vividly shown in Figure 3b. Note that two more dangling bonds are saturated with a hexagon formation, and therefore this geometry is very stable with a complete

(17) Lee, Y. H.; Kim, S. G.; Tomanek, D. *Phys. Rev. Lett.* **1997**, *78*, 2393.

(18) Oh, D.-H.; Lee, Y. H. *Phys. Rev. B* **1998**, *58*, 153.

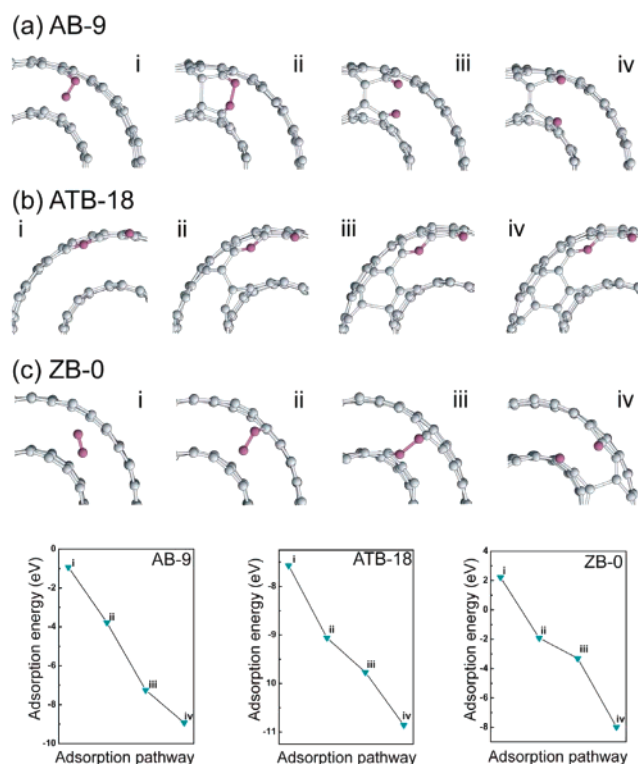


Figure 3. Concerted pathways of some important bridged structures during exothermic adsorption and the related energetics.

hexagon formation near the bridged hexagon and, in particular, the dimer bond length of the bridged atoms is 1.49 Å, leading to a large energy gain of -10.9 eV. The relative orientation plays an important role in forming a bridged hexagon in this case, where such geometry is not found in other orientations. We next consider O_2 adsorption on a zigzag DWCNT edge. Figure 2g is a reference geometry with an adsorption energy of -8.32 eV, where O_2 was adsorbed exothermically on the inner top sites. This has been reported to be the most stable with an adsorption energy of -8.29 eV.⁶ The adsorption of O_2 molecule at the outer top sites gives slightly stronger energy of -8.43 eV due to the strain energy difference between two tube walls. When an O_2 molecule was placed above two top sites with the molecular axis parallel to the radial direction, it dissociates exothermically into two top sites at both walls, as shown in Figure 2h. The adsorption energy is -8.74 eV, slightly larger due to the weak O–O repulsive energy. The least strain energy is retained in this geometry. The situation is different when an O_2 molecule was placed between the middle of two top sites with the molecular axis oriented by 45° from the radial direction. This induces lip–lip interactions again similar to those in armchair tubes (ZB-0). One oxygen atom of O_2 molecule first forms a C–O bond with the edge carbon atom at the outer wall, gaining about -2 eV, as shown in step (ii) of Figure 3c. The next step is to pull out another carbon edge atom of the inner wall, eventually forming C–O bond, as shown in step (iii). This process activates the adjacent C–C bridge formation, and as a consequence the O–O bond is dissociated.

The bridged dimer forms a double bond with a bond length of 1.39 Å. We note that the Mulliken charges at oxygen atoms are always greater in the bridged geometries compared to other unbridged geometries, suggesting that the Mulliken charge-transfer plays an important role in forming lip–lip interactions.

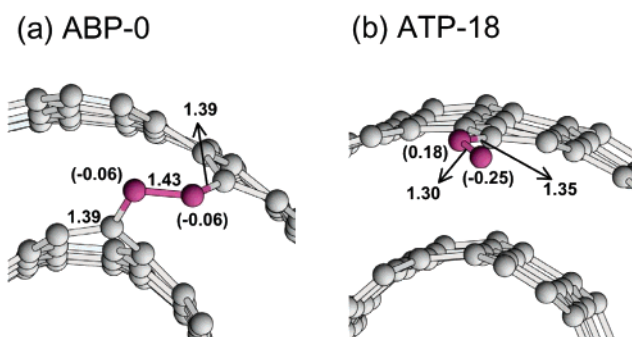


Figure 4. Bird's eye view of some O_2 molecular precursor states. (a) A "bridged precursor" at armchair edge, (b) "on-top precursor" at armchair edge.

Table 2. Some O_2 Molecular Precursor States Which Exist on DWCNT Edges^a

type	E_{ad} (eV)	l_{oo} (Å)	l_{co} (Å)	δC (e)
ABP-0	-3.31	1.43	1.39	$-0.06, -0.06$
ATP-18	-2.00	1.30	1.35	$-0.18, -0.25$

^a All notations are similar to those in Table 1.

The adsorption energy is -9.91 eV, which is a large energy gain again due to the smaller strains in this geometry. We have also tried various orientations with different adsorption geometries. However, all stable structures belong to the current categories of geometries listed in Figure 2. To check the accuracy of our SCC-DFTB calculations, we performed the LDA calculations for some stable geometries. Table 1 shows that the LDA calculations give larger adsorption energies than the SCC-DFTB calculations in all cases. However, the SCC-DFTB energetics basically follow the LDA energetics, confirming the validity of our approaches with the SCC-DFTB.

So far we have described the edge interactions with strong chemisorption induced by an O_2 molecule. In addition to these, we find that several O_2 molecular precursor states exist at the DWCNT edge. Figure 4a shows an O_2 molecular precursor at armchair edge, where O_2 molecule is bridged between the middle of two dimers with the molecular axis deviated by 45° from the radial direction. The O–O bond length is extended to 1.43 Å, longer than the molecular bond length of 1.21 Å. The Mulliken charge transfer is -0.06 at the oxygen atom, much smaller than that of the strongly chemisorbed cases. We note that this configuration is stable with strong C–O bonds with an l_{CO} of 1.39 Å, which is a double bond.

The adsorption energy is -3.31 eV, still much weaker than those of strongly chemisorbed geometries via the bridged lip–lip interactions but could be regarded as a chemisorption. We find another O_2 precursor state either at the outer wall or inner wall, as shown in Figure 4b. The O–O distance is extended to 1.30 Å. The adsorption energy is -2.0 eV due to a strong l_{CO} of 1.35 Å, which can be again regarded as a chemisorption. Those optimized parameters of precursor states are summarized in Table 2. The open tube edges can be stable at low temperature. At high temperature the tube edge starts interacting, leading to formation of a capped structure or a closed tube end.^{19,20} In the presence of oxygen gases, the cap closure can be accelerated even at room temperature²¹ due to the adsorbate-induced lip–lip interactions via bridged atoms as shown in our

(19) Charlier, J. C.; Vita, A. D.; Blasé, X.; Car, R. *Science* **1997**, *275*, 647.

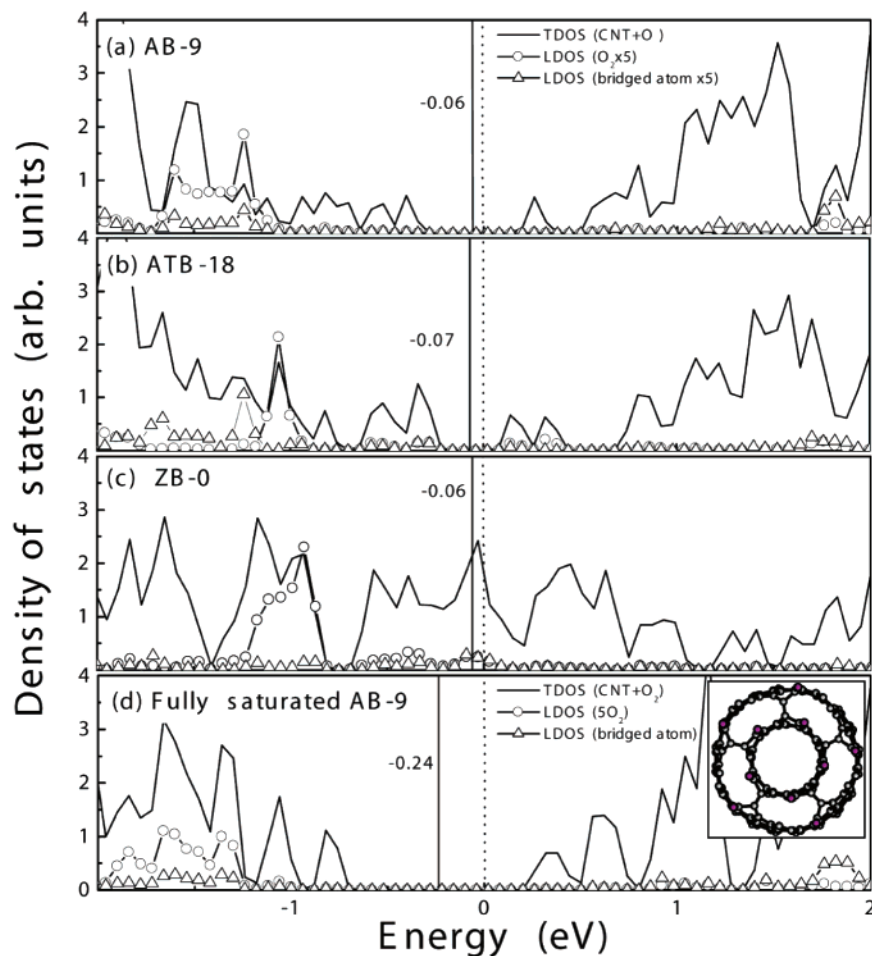


Figure 5. Electronic density of states for most stable adsorption geometries of (a) AB-9, (b) ATB-18, (c) ZB-0, and (d) fully saturated AB-9 which is shown in the inset. The solid line indicates the total density of states; open circles and open triangles indicate the magnified local density of states from adsorbed oxygen molecule and the bridged atom, respectively.

report. Therefore the SWCNT model is not appropriate in explaining the field emission characteristics of the DWCNT or MWCNT. The adsorbate-induced lip–lip interactions can also explain why the MWCNT and DWCNT tips are more stable than the SWCNT tip in the field emission; i.e., the saturated dangling bonds at the DWCNT edges reduce an oxidative etching rate compared to the open SWCNTs, particularly at high fields, in excellent agreement with experimental observations.^{10,22}

Electronic Structure. One of the crucial factors in the field emission currents is the work function, which is directly proportional to the Fermi level shift.²³ Figure 5 shows the local electronic density of states (LDOS) for various stable geometries. The Fermi level shifts toward the valence band by 0.06 eV in the armchair (AB-9) tube in Figure 5a. This shift is smaller than that of the open SWCNT edge.⁹ No LDOS is available at the Fermi level. This trend is similar in another type (ATB-18), as shown in Figure 5b. The Fermi level shift is also very

small in zigzag edges. However, we note that the LDOS at the Fermi level exists in the zigzag tube, as shown in Figure 5c. The contribution from the bridged atoms is not negligible.

The Fermi level shift at a complete saturation of the tube edge by O₂ molecules in the AB-9 model is -0.24 eV, simply close to the multiplication of the number of the bridged sites. The contribution from the oxygen adsorbates is negligible. From this point of view, the field emission from DWCNTs is very different from that from SWCNTs. The change of the Fermi level in the DWCNT is less than that in the SWCNT, and therefore we expect the emission current to be larger in the DWCNT or MWCNT than in the SWCNT. This agrees well with experimental observations.^{22,24} Furthermore, an O₂ molecule does not contribute to the localized gap states particularly in armchair tubes.

Summary

In summary, we have investigated an adsorption of an O₂ molecule on DWCNT edges using DF calculations. Although several O₂ precursor states exist, O₂ adsorbs exothermically with no activation barrier on DWCNT edges in most cases. Moreover, adsorption of an O₂ molecule induces spontaneous lip–lip

(20) Andrew, J. L.; Rinzler, G.; Dai, H.; Hafner, J. H.; Bradley, R. K.; Boul, P. J.; Lu, A.; Iverson, T.; Shelimov, K.; Huffman, C. B.; Macias, F. R.; Shon, Y. S.; Lee, T. R.; Colbert, D. T.; Smalley, R. E. *Science* **1998**, *280*, 1253.

(21) Chang, J. Y.; Ghule, A.; Chang, J. J.; Tzing, S. H.; Ling, Y. C. *Chem. Phys. Lett.* **2002**, *363*, 582.

(22) Bonard, J.-M.; Salvétat, J.-P.; Stockli, T.; de Heer, W. A.; Forro, L.; Chatelain, A. *Appl. Phys. Lett.* **1998**, *73*, 918.

(23) Chen, C. W.; Lee, M. H. *Diamond Relat. Mater.* **2003**, *12*, 565.

(24) Chung, D. S.; Choi, W. B.; Kang, J. H.; Kim, H. Y.; Han, I. T.; Park, Y. S.; Lee, Y. H.; Lee, N. S.; Jung, J. E.; Kim, J. M. *J. Vac. Sci. Technol., B* **2002**, *18*, 1054.

interactions, forming the closed tube ends. This shows why the MWCNT or DWCNT tips are more stable than the SWCNT tip in the field emission. We have also calculated the electronic density of states for stable adsorption geometries. O₂ adsorption shifts the Fermi level toward the valence bands similar to that of the SWCNT, but the change in the Fermi level is much smaller, giving rise to a large field emission current in the DWCNT. The adsorbed oxygen molecule does not contribute

to the field emission currents in armchair tubes, since the localized oxygen states are located away from the Fermi level.

Acknowledgment. This work was supported by the MOST through the NRL program and in part the KOSEF through the CNNC at SKKU. We thank to the computer center of Chonbuk National University for the computing resources.

JA039917Z